

# Wavelet Analysis in Soliton Detection

Mark A. Coffey, Delores M. Etter

Colorado Center for Astrodynamics Research  
Department of Electrical and Computer Engineering  
University of Colorado  
Boulder, CO 80309 USA

**Abstract** — The structure of arbitrary wavelet bases derived from the generalized  $B$ -spline wavelets is introduced. An arbitrary wavelet basis is constructed and then used to detect the presence of dynamic solitons in the sea surface height as measured by satellite altimetry. Comparisons are made for wavelet decompositions based on several scaling functions.

## I. INTRODUCTION

The discrete wavelet transform (DWT) is uniquely qualified as a detection algorithm for digital signals. The transform, properly designed, is inherently localized in both time and frequency, and as such is a valuable tool when analyzing non-periodic data. The DWT decomposes a given signal into a series of orthogonal wavelet subspaces. This decomposition preserves energy relationships between the subspaces, and the DWT can even be designed so as to be orthogonal within each individual subspace. There is a great deal of freedom that can be exploited in the DWT, as the choice of the actual wavelet is an underdetermined problem in the proper setting. We seek to optimize the structure of the DWT for detection by examining the formation of arbitrary wavelet bases that are ideally suited to the detection of a given signature waveform.

In order to illustrate the utility of the DWT in detection, we will consider the analysis of satellite remote-sensing data over the ocean. In contrast to conventional shipboard data-gathering techniques, satellite altimetry yields a more comprehensive global representation of such phenomenon as the sea surface height (SSH) of the world's oceans. Ocean dynamics dictate that this data will be highly non-linear and time-variant, conditions in which conventional signal processing techniques may fail. We consider the construction of an appropriate wavelet basis to analyze transient oceanic signals and then apply the analysis to along-track SSH data in order to detect the presence of non-linear waves called solitons in the Sulu Sea.

## II. CONSTRUCTION OF THE WAVELET BASIS

While Fourier analysis decomposes signals in terms of sinusoids, wavelet analysis expands this idea to include decompositions based on large families of localized basis functions. These wavelets satisfy several well-documented [1-3] properties, including the fact that the basis functions are relatively isolated in both time and frequency. The most well-known wavelets are those constructed by Daubechies, denoted as  $\psi_p^n$ , which are compactly supported in time and are orthogonal to one another within and across the wavelet subspaces [2]. It can be shown that the Daubechies wavelets

are but a subclass of a more generalized framework proposed by Chui [3]. Building upon a generalized Bernstein-spline ( $B$ -spline) structure, this framework generates many wavelet bases that may be constructed with any number of design goals in mind, including, among others, compactly-supported bases and causal filter implementations. Wavelets exhibit dilation properties which ensure that the representation of any discrete signal at some resolution level is determined from the representation at the next finer resolution level. The entire transform may thus be implemented with an efficient filter bank [4].

The core of the detection problem is to identify and locate a given signature pattern within an arbitrary data sequence. For periodic signals, Fourier analysis lends itself to accurate and efficient identification algorithms. However, for localized (and thus non-periodic) signals hidden in a much larger data sequence, Fourier analysis falls far short of solving the detection problem. Wavelet analysis, on the other hand, offers a much more natural approach to such problems. Given the infinite number of wavelet bases that are available, the challenge then becomes to identify and construct the wavelet that will most effectively solve the detection problem.

We will build upon the  $B$ -spline representation for the scaling function and wavelet in order to construct a wavelet best suited to the detection process. Wherever possible, we will adhere to Chui's notation.

A fundamental result of interpolation theory states that any function residing in  $\pi_m$ , the space of polynomials of order  $m$ , can be generated using the corresponding  $B$ -spline of order  $m$  [5]. These spline functions are constructed as the  $m$ -fold convolution of the characteristic function with itself:

$$\beta^m(x) = \beta^0 * \beta^{m-1}(x); \quad \beta^0(x) = 1, \quad x \in [0,1] \quad (1)$$

We can choose as our scaling function  $\phi(x)$  any one of the  $B$ -splines. Since the splines themselves form a basis for the fundamental space  $V_0$ , a linear combination of them will also form a basis. The associated two-scale symbol  $P(z)$  is

$$P(z) = \left(\frac{1+z}{2}\right)^m S(z) \quad (2)$$

Generally,  $S(z)$  is chosen to be unity so that the associated two-scale sequence  $\{p_n\}$  is of minimum compact support, resulting in the cardinal  $B$ -spline scaling function of order  $m$ . From the scaling function, the remaining two-scale symbols  $Q(z)$ ,  $G(z)$ , and  $H(z)$  are constructed so that the properties of the wavelet transform are satisfied. In particular, the wavelet function has as its two-scale symbol

$$Q(z) = z^{-1}E(-z)\bar{P}(-z^{-1})E^{-1}(z^2)K(z^2) \quad (3)$$

where  $E(z)$  is the Euler-Frobenius polynomial associated with the  $B$ -spline and  $K(z)$  is restricted to the Wiener class  $W$ , the class of Laurent series in  $z$  for which the corresponding sequences are in  $\ell_1$ . This implies that  $f \in W \Rightarrow f(z) \neq 0, |z|=1$ . In constructing the cardinal  $B$ -spline wavelets, choose  $K(z)$  so that the resulting  $Q(z)$  (and hence  $\psi(x)$ ) has minimum support:

$$\begin{aligned} K(z) &= -zE(z) \\ Q(z) &= -zE(-z)\bar{P}(-z^{-1}) \end{aligned} \quad (4)$$

However, this restriction on  $K(z)$  is unnecessarily harsh. In fact, we can use the additional freedom in the choice of  $K(z)$  to construct a wavelet which will best satisfy the detection problem. In particular, the new wavelet should resemble as closely as possible the signature waveform, so that the resulting coefficients in the DWT will be maximized when the signature is encountered in the data stream.

Before formulating the problem of constructing the new wavelet, let us first examine the means by which the scaling and wavelet functions are generated by the two-scale sequences  $\{p_n\}$  and  $\{q_n\}$ . By definition, the continuous functions at resolution level  $j$  are given by convolution of the function at the  $(j-1)$ <sup>th</sup> level with the two-scale sequence:

$$\phi(x) = \sum_n p_n \phi(2x-n), \quad \psi(x) = \sum_n q_n \phi(2x-n) \quad (5)$$

(During the analysis of the signal, we assume that the signal originates in  $V_0$ , the space corresponding to  $j=0$ , with the subspaces becoming more coarse as  $j$  decreases. Thus  $j \in \{0, -1, -2, \dots\}$ .) When iterated, equation (5) translates into an algorithm by which the integer values of  $\phi(x)$  and  $\psi(x)$  at any resolution level may be calculated. Define

$$\phi(x)|_{x=n} \xleftrightarrow{z} \Phi_0(z) \quad (6)$$

as the  $z$ -transform of the scaling function at the root resolution level  $j=0$ , sampled at the integers. Then for  $j=-1$  equation (5) is equivalent to

$$\phi(2^{-1}x)|_{2^{-1}x=n} \xleftrightarrow{z} \Phi_{-1}(z) = \Phi_0(z)P(z) \quad (7)$$

By induction, at the  $j$ <sup>th</sup> resolution level we have

$$\phi(2^j x)|_{2^j x=n} \xleftrightarrow{z} \Phi_j(z) = \Phi_0(z) \prod_{n=0}^{|j|-1} P(z^{2^n}) \quad (8)$$

for  $j < 0$ . Similarly, the representation for  $\psi(x)$  at the  $j$ <sup>th</sup> resolution level is

$$\begin{aligned} \psi(2^j x)|_{2^j x=n} &\xleftrightarrow{z} \Psi_j(z) \\ \Psi_j(z) &= \Phi_0(z)Q(z^{2^{|j|-1}}) \prod_{n=0}^{|j|-2} P(z^{2^n}) \end{aligned} \quad (9)$$

Once the cardinal  $B$ -spline wavelet has been constructed, we can create an entire class of wavelets which generate the same signal subspace by taking an invertible linear combination of the original wavelet. In our framework, we would like this new wavelet  $\tilde{\psi}(x)$  to resemble the detection signature as closely as possible at a given resolution level. This new wavelet must also satisfy a two-scale relation, and

so we redefine not the wavelet itself but the two-scale relation which generates it. This is the equivalent of choosing  $K(z)$  in equation (3) as

$$K(z) = -zE(z)\tilde{K}(z), \quad \tilde{K}(z) \in W \quad (10)$$

The new wavelet at a given resolution level  $j$  is then

$$\begin{aligned} \tilde{\psi}(2^j x)|_{2^j x=n} &\xleftrightarrow{z} \tilde{\Psi}_j(z) \\ \tilde{\Psi}_j(z) &= \Phi_0(z)[\tilde{K}Q](z^{2^{|j|-1}}) \prod_{n=0}^{|j|-2} P(z^{2^n}) \end{aligned} \quad (11)$$

$\tilde{K}(z)$  is now in terms of dilated powers of  $z$ . Expressed in the time domain,

$$\tilde{\psi}(2^j x)|_{2^j x=n} = \{\tilde{k}_n\}_{\uparrow 2^{-j}} * \psi(2^j x)|_{2^j x=n} \quad (12)$$

Since  $\{\tilde{k}_n\}_{\uparrow 2^{-j}}$  is upsampled  $|j|$  times, the majority of the coefficients in this sequence are fixed and equal to zero. For example, let  $j=-1$  be the resolution level at which we want to approximate the signature waveform. Expressed in matrix form, (12) becomes:

$$\begin{bmatrix} \psi_0 & 0 & 0 & 0 & 0 & 0 \\ \psi_1 & 0 & 0 & 0 & 0 & 0 \\ \psi_2 & \psi_0 & 0 & 0 & 0 & 0 \\ \psi_3 & \psi_1 & 0 & 0 & 0 & 0 \\ \psi_4 & \psi_2 & \psi_0 & 0 & 0 & 0 \\ \psi_5 & \psi_3 & \psi_1 & 0 & 0 & \ddots \end{bmatrix} \begin{bmatrix} \tilde{k}_0 \\ \tilde{k}_1 \\ \tilde{k}_2 \\ \tilde{k}_3 \\ \tilde{k}_4 \\ \vdots \end{bmatrix} = \begin{bmatrix} \tilde{\psi}_0 \\ \tilde{\psi}_1 \\ \tilde{\psi}_2 \\ \tilde{\psi}_3 \\ \tilde{\psi}_4 \\ \vdots \end{bmatrix} \quad (13)$$

where  $\tilde{\psi}_n$  are the samples of the signature waveform at the integers and

$$\psi_n = \psi(2^j x)|_{2^j x=n}, \quad n \in \mathbb{N}$$

are the elements of the convolution matrix. Note that since the constrained coefficients in the vector  $\mathbf{k}$  are zero, we retain only every  $(2^j)$ <sup>th</sup> column from the standard convolution matrix. In more concise form, this reduces to

$$\mathbf{R}\mathbf{k} = \tilde{\Psi} \quad (14)$$

Inversion of the convolution matrix  $\mathbf{R}$  is an ill-conditioned problem if there are roots on the unit circle. This becomes a key consideration in attempting to solve equation (14) for  $j=0$ . In general, the  $B$ -splines produce wavelets whose sampled versions will necessarily have roots on the unit circle. In fact, by substituting in for the cardinal form of  $P(z)$  in the equation for  $\Psi(z)$ , we have

$$\begin{aligned} \tilde{\Psi}_j(z) &= \Phi_0(z)[\tilde{K}Q](z^{2^{|j|-1}}) \prod_{n=0}^{|j|-2} P(z^{2^n}) \\ &= A(z)\tilde{K}(z^{2^{|j|-1}}) \left(1 + z^{-2^{|j|-1}}\right)^m \prod_{n=0}^{|j|-2} (1 - z^{2^n})^m \end{aligned} \quad (15)$$

with  $A(z) \in W$ . Equation (15) contains  $(j-1)m$  roots at  $z=-1$  and  $(j-2)!m^{j-2}$  roots at  $z=1$ . Since this equation holds even for the most generalized form of the  $B$ -spline family of wavelets, it would seem that there is no guaranteed solution to the problem. However, the subsampling of the

matrix in (13) for  $j < 0$  stabilizes the problem. Note that  $\mathbf{R}$  is never square and therefore not invertible in the usual sense. The problem is best solved using the Moore-Penrose pseudoinverse of  $\mathbf{R}$ , which results in the minimum error-energy (least-squares) fit to  $\tilde{\psi}(x)$  [7].

$$\tilde{\mathbf{k}} = \mathbf{R}^+ \tilde{\Psi} = (\mathbf{R}^* \mathbf{R})^{-1} \mathbf{R}^* \tilde{\Psi} \quad (16)$$

where  $\mathbf{R}^*$  denotes the conjugate transpose. Having solved for  $\tilde{\mathbf{K}}(z)$ , form a two-scale symbol for the new wavelet as

$$\begin{aligned} Q_{\text{new}}(z) &= \tilde{\mathbf{K}}(z) Q(z) \\ &= -z \tilde{\mathbf{K}}(z) E(-z) \bar{P}(-z^{-1}) \end{aligned} \quad (17)$$

The new wavelet is guaranteed to satisfy the properties of the wavelet transform and should make an ideal detector for the signature waveform with which it was designed.

We next turn to the formation of a wavelet basis for the detection of solitons in satellite altimeter data. The method outlined in this section will be used to create a new wavelet, and then the resulting wavelet transform will be applied.

### III. INTERNAL WAVES AND SOLITONS IN THE SULU SEA

The Sulu Sea presents a unique opportunity for the detection of solitons in the ocean's surface signature. Located just to the southwest of the Philippines, the sea is bordered by land masses which harbor and then deflect large internal (sub-surface) waves according to the tidal currents present in the area. These large-amplitude internal waves create smaller-amplitude surface waves called solitons which should be detectable by satellite remote-sensing of the SSH [7]. We use data from the TOPEX/Poseidon satellite mission, which is equipped with an on-board altimeter capable of millimeter-precision measurement of the SSH along satellite tracks.

Solitons are isolated waves which travel independently of each other or other oceanic waves. Based on empirical analysis, oceanographers are able to model solitons as

$$z(x, t) = \frac{4}{3} A \text{sech}^2 \left[ \sqrt{A} \left( x \pm \frac{3+2A}{3} t + x_0 \right) \right] \quad (18)$$

where  $x$  is the distance along track,  $t$  is the time since inception, and  $A$  is a constant that depends on the surface wave amplitudes [8]. Fig. 1 illustrates a wave train composed of three solitons generated from this model.

Solitons create a non-linear signal of relatively short duration which can easily become lost in surface noise or large-amplitude signals. In order to detect the presence of

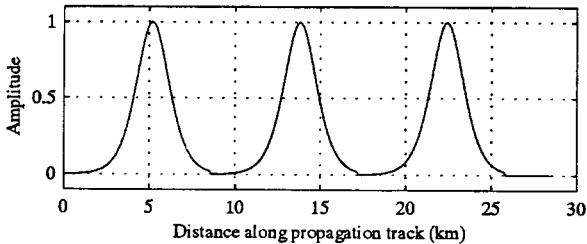


Fig. 1. Soliton wave train based on analytical modeling. The TOPEX altimeter samples this signal at 10Hz (approx.  $1/57\text{km}^{-1}$ ).

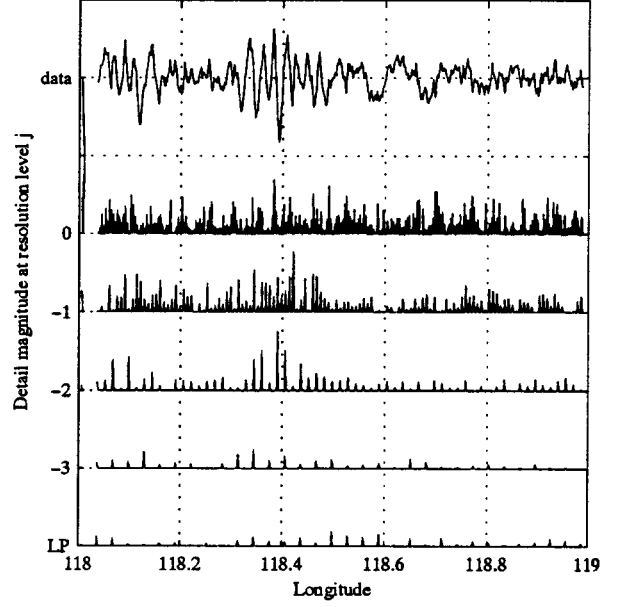


Fig. 2. DWT of the SSH over the Sulu Sea using Daubechies' wavelet of order 4. The original data is shown at the top, with detail signals displayed below. Longer wavelength signals show up in the lower levels of the transform. The final projection onto the coarsest subspace (LP) is at the bottom.

these solitons, the SSH data was transformed using a conventional Daubechies' wavelet of order 4. The resulting wavelet decomposition is shown in Fig. 2.

The original signal is shown at the top of the figure. Decreasing levels correspond to the detail signal at coarser resolution levels (lower-frequency projections). From the magnitudes of the detail signals in the figure, we can see several good candidates for soliton wave trains identified in the SSH, one most notably at approximately  $118.4^\circ$  longitude. The wave train appears mostly in the detail signals corresponding to  $j=0$  and  $j=-1$ , indicating that the energy present in the solitons is spread out over a larger frequency band and is not localized optimally by the decomposition. In addition, the noise level is rather high on the resolution levels where the soliton train shows up, making for less reliable detection.

The Daubechies wavelet does a reasonable job of identifying the wave train. However, a plot of the actual  $\psi_d^4$  wavelet (Fig. 3) shows that it does not bear as much resemblance to the soliton as it might. The wavelet decomposition performs better with basis functions that

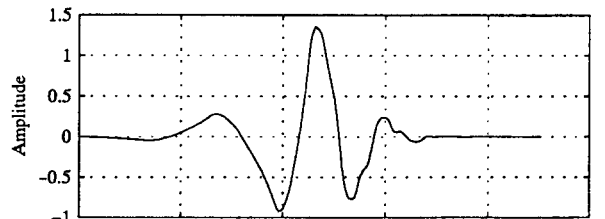


Fig. 3.  $\psi_d^4$  wavelet used for the decomposition in Fig. 2.

closely resemble the signal of interest. With this in mind, an arbitrary wavelet may be constructed to form a more optimal decomposition.

A new wavelet is constructed using the method outlined in Section III. First, the cardinal  $B$ -spline scaling function and wavelet of order 4 are constructed as in Chui. We then pick a resolution level at which we would like to see most of the soliton train energy appear, say  $j=-1$ . Calculate the discrete samples of  $\psi_u$ , and then form the matrix  $\mathbf{R}$  as in equation (14). Take  $\tilde{\Psi}$  to be a vector of values from the analytical model of the soliton wave train in Fig. 1 sampled at the same rate as that of the satellite altimeter (10Hz for the TOPEX altimeter). Calculate the pseudoinverse of  $\mathbf{R}$  in order to solve for  $\mathbf{k}$ . The new two-scale sequence,  $\tilde{K}(z)Q(z)$ , yields the new wavelet. Fig. 4 shows the cardinal  $B$ -spline scaling function and wavelet of order 4, the analytical soliton train from Fig. 1, and the new wavelet. The agreement between the new wavelet and the soliton train is remarkably good, with a mean-squared error of  $1.2 \times 10^{-3}$  between the samples of the two functions.

Using the new two-scale sequences, the SSH data is passed through the DWT and the results are shown in Fig. 5. As expected, the localization of the soliton train is now much more pronounced against the background noise.

In constructing the new wavelet, it is generally in the best interest of the designer to ensure that the signature waveform resides at least partly in the subspace generated by the original cardinal  $B$ -spline wavelet. It is unrealistic to expect the transform to concentrate energy from a signal with a large mean into any one (or even several) wavelet subspaces. Note in Fig. 4 that the low-frequency components of the soliton wave train have been removed prior to constructing the new wavelet. Also, we require  $\tilde{K}(z) \in W$  in order for the wavelet transform to be fully reversible, although equation (16) does not guarantee such a condition. Since we can factor a minimum-phase equivalent for  $\tilde{K}(z)$ , the only problem that may arise is when roots of the polynomial have magnitude close to one, in which case the synthesis filter  $H^*(z)$  will become unstable. In the detection problem, however, we are generally not concerned with reconstructing the signal once it has been decomposed.

#### IV. CONCLUSIONS

Wavelet analysis proves to be increasingly useful in

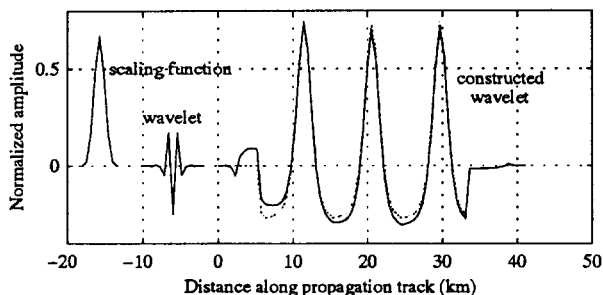


Fig. 4. Construction of the new wavelet basis. At left are shown the cardinal  $B$ -spline scaling function and wavelet of order 4. The dotted wave to the right is the soliton train from Fig. 1, and the solid line is the newly-constructed wavelet.

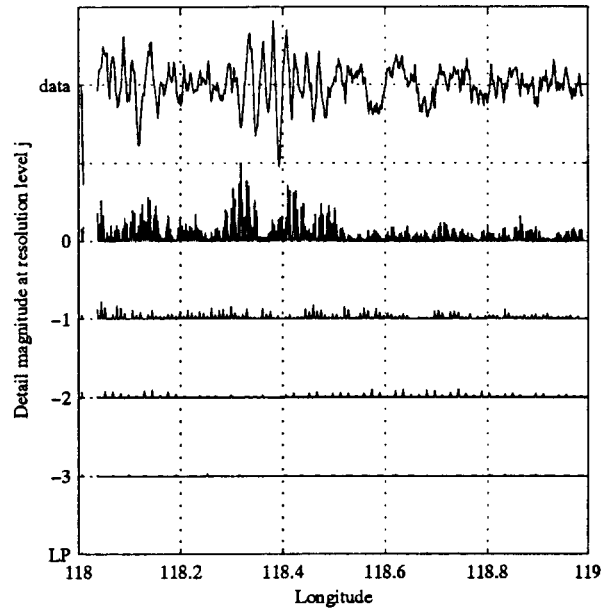


Fig. 5. Discrete wavelet transform of the same SSH data using the constructed wavelet. Note the pronounced localization of the wave train energy in the transform at  $j=0$ . Signal noise is suppressed much better with the new wavelet.

applications dealing with inherently time-variant, dynamic systems. The wavelet decomposition lends itself to a considerable amount of diversity, since it can be based on a large family of mother wavelets, with consideration made for such practical implementation issues as stability and causality. The  $B$ -splines make particularly useful basis wavelets from which to construct wavelets more appropriate to the detection problem. Comparisons done on actual data confirm that the new wavelets perform better under the detection criterion than such standard wavelets as the Daubechies' or the cardinal  $B$ -splines wavelets.

#### V. REFERENCES

- [1] Ali N. Akansu and Richard A. Haddad, Multiresolution Signal Decomposition, Academic Press, 1992.
- [2] Ingrid Daubechies, Ten Lectures on Wavelets, Society for Industrial and Applied Mathematics, Philadelphia, PA, 1992.
- [3] C. K. Chui, An Introduction to Wavelets, Academic Press, San Diego, CA, 1992.
- [4] Stephen Mallat, "A theory for multiresolution signal decomposition: the wavelet representation" *IEEE Trans. Pattern Anal. and Machine Intell.* vol. 11, n. 7, July 1989.
- [5] Michael Unser and Akram Aldroubi, "Polynomial splines and wavelets - a signal processing perspective," *Wavelets - A Tutorial in Theory and Application*, C.K. Chui, ed., Academic Press, 1992.
- [6] Richard Roberts and Clifford Mullis, Digital Signal Processing, Addison-Wesley, 1987.
- [7] John R. Apel, James R. Holbrook, et al., "The Sulu Sea Internal Soliton Experiment," *Journal of Physical Oceanography*, v. 15, p. 1625, December 1985.
- [8] A. R. Osbourne and T.L. Burch, "Internal solitons in the Andaman Sea," *Science*, v. 208, n. 4443, May 1980.